Research Article

3D Fluid-Dynamic Ovarian Cancer Model Resembling Systemic Drug Administration for Efficacy Assay

Alessandra Marrella[1], Gabriele Varani[1], Maurizio Aiello[2], Ivan Vaccari[1], Chiara Vitale[1], Martin Mojzisek[3], Cristina Degrassi[3] and Silvia Scaglione[1,2]

[1]CNR – National Research Council of Italy, IEIIT Institute, Genoa, Italy; [2]React4life S.r.l, Genoa, Italy; [3]MTTlab S.r.l, Trieste, Italy

Abstract

Recently, 3D *in vitro* cancer models have become important alternatives to animal tests for establishing the efficacy of anticancer treatments. In this work, 3D SKOV-3 cell-laden alginate hydrogels were established as ovarian tumor models and cultured within a fluid-dynamic bioreactor (MIVO®) device able to mimic the capillary flow dynamics feeding the tumor. Cisplatin efficacy tests were performed within the device over time and compared with (i) the *in vitro* culture under static conditions and (ii) a xenograft mouse model with SKOV-3 cells, by monitoring and measuring cell proliferation or tumor regression, respectively, over time. After one week of treatment with 10 μM cisplatin, viability of cells within the 3D hydrogels cultured under static conditions remained above 80%. In contrast, the viability of cells within the 3D hydrogels cultured within dynamic MIVO® decreased by up to 50%, and very few proliferating Ki67-positive cells were observed through immunostaining. Analysis of drug diffusion, confirmed by computational analysis, explained that these results are due to different cisplatin diffusion mechanisms in the two culture conditions. Interestingly, the outcome of the drug efficacy test in the xenograft model was about 44% of tumor regression after 5 weeks, as predicted in a shorter time in the fluid-dynamic *in vitro* tests carried out in the MIVO® device. These results indicate that the *in vivo*-like dynamic environment provided by the MIVO® device allows to better model the 3D tumor environment and predict *in vivo* drug efficacy than a static *in vitro* model.

1 Introduction

Ovarian cancer is one of the main causes of death in female cancer patients (Sankaranarayanan and Ferlay, 2006). The poor survival rate is mainly due to chemoresistance to established drug protocols, as also happens in many other cancer cases (Lowe et al., 2013). In this context, the increasing prevalence of drug-resistant cancers necessitates further research and treatment development. Currently, an anticancer drug candidate that enters Phase I trials will successfully proceed further with a probability of only 8%, highlighting the urgent need for new physiologically relevant *in vitro* tumor models better resembling the *in vivo* conditions to test novel drugs and therapies (Suggitt and Bibby, 2005).

Based on current regulatory guidelines, screening of new cancer drugs is carried out by using high-throughput assays, where *in vitro* toxicity and efficacy tests are performed on cells grown as monolayers over planar plastic surfaces; then, in preclinical development, *in vivo* toxicological and ADME (adsorption, distribution, metabolism, excretion) studies are performed in animal models. However, it is now widely demonstrated that 2D cell cultures are oversimplified and poorly resemble the complex 3D tumor microenvironment (Abbott, 2003; Loessner et al., 2010; Marrella et al., 2019). On the other hand, animal models commonly fail to predict human safety and efficacy in clinical studies, besides being expensive and associated with ethical issues (Liu et al., 2013). Therefore, in the last years, novel human 3D *in vitro* culture systems have increasingly gained attention as potential compromises between traditional 2D cultures and *in vivo* models (Hoarau-Véchot et al., 2018). They aim to combine the advantages of the former (better control of the experimental conditions, relative ease of manipulation and analysis, species-specificity) and approach the latter by better representing *in vivo* physiology.

In this scenario, 3D tumor spheroids have been proposed as *in vitro* human cancer models (Raghavan et al., 2015; Herter et al., 2017). Spheroids are scaffold-free aggregations of cells suitable for prolonged *in vitro* culture and high-throughput drug testing.

Received March 13, 2020; Accepted July 8, 2020;
Epub August 3, 2020; © The Authors, 2020.

ALTEX 38(1), 082-094. doi:10.14573/altex.2003131

Correspondence: Silvia Scaglione, PhD
via de Marini 6
16149 Genova, Italy
(silvia.scaglione@ieiit.cnr.it)

They have been shown to resemble many physiological aspects better than cells grown in monolayers (e.g., physical borders, chemical gradients) (Thoma et al., 2014). The cells exhibit cell-cell interactions in all spatial directions, resembling shapes and phenotypes close to those observed *in vivo*. Moreover, the cancer cell proliferation rate within spheroids has been found to be comparable with that observed *in vivo*, which is substantially lower than that of cells cultured in 2D conditions (Longati et al., 2013). Depending on the tumor cell types and cell packing densities, tumor spheroids with diameters of up to 600 µm can be generated (Xu et al., 2014). They are particularly suitable to model ovarian cancer, since ovarian cancer cells grow as spheroids in some patients (Burleson et al., 2004).

Although these 3D culture systems have widely improved the reliability of *in vitro* tests in different oncologic areas, they still have some limitations, particularly due to a lack of surrounding extracellular matrix (ECM). For example, cell-based models are susceptible to physical disintegration during manipulation; moreover, microenvironmental conditions, for example cell-ECM interactions and matrix mechanical rigidity, cannot be finely tuned (Markovitz-Bishitz et al., 2010). Furthermore, the mass transport and the kinetics of the release of anticancer drugs in solid tumors cannot be accurately replicated due to the non-uniform secretion of endogenous extracellular matrix by the spheroids.

Therefore, 3D scaffold-based cancer models able to resemble the function of the ECM have been investigated and recently developed. Tumor-associated stromal ECM is in fact an important component of the tumor microenvironment, playing crucial roles in cancer progression and invasion (Weaver and Roskelley, 1997; Dutta and Dutta, 2009). Tumor cells can be either encapsulated into hydrogels, bioprinted in 3D matrixes or cultured embedded in artificial membranes/scaffolds. The association of cancer cells with an artificial ECM allows to more closely recapitulate pathophysiological features of native tumor tissues (Hutmacher et al., 2010), improving the understanding of the reciprocal interactions between the tumor cells and their surrounding microenvironment, which physiologically includes the stromal ECM molecules, immune cells, stromal cells, as well as growth factors and cytokines (LaBarbera et al., 2012).

Polymeric materials (mainly hydrogels) are used as artificial ECM (Nyga et al., 2011; Fang and Eglen, 2017; Marrella et al., 2018). They are matrices in which tumor cells can be encapsulated to then proliferate, migrate and arrange (Nicodemus and Bryant, 2008; Marrella et al., 2017). These hydrogel-based models have provided new methods for accelerating cancer research, in particular improving the quality of preclinical cancer research (Jiguet Jiglaire et al., 2014). In fact, these 3D matrix-assisted cancer models support more complex cell-cell and cell-ECM interactions, leading to biochemical signals and mechanical forces that can influence cell motility, proliferation and gene expression (Huber et al., 2016).

Matrix-assisted tumor models also can be derived from patient biopsies or explants, named organoids, allowing the *ex vivo* propagation of tumors from individual patients; the organoids are also able to self-organize to resemble organ function (Clevers, 2016). Although standard protocols for their maintenance in culture are not yet available (Weeber et al., 2017) and their manipulation requires a specific expertise (patient cell isolation can be challenging in terms of sterility and cell expansion), these systems are valuable for the *in vitro* analysis of those types of cancers for which there are no immortalized cell lines (Brancato et al., 2020).

If originally the term organoid referred to primary cultures of tissue fragments separated from the stroma within 3D gels to form organ-like structures (Simian and Bissell, 2017), now the term organoid refers to a wide range of techniques for the *in vitro* culture of self-organizing and self-renewing 3D cultures obtained from primary tissue, embryonic or induced pluripotent stem cells, whose functionality recapitulates that of the tissue from which they have been extracted (Lancaster and Knoblich, 2014; Shamir and Ewald, 2014; Fatehullah et al., 2016; Kretzschmar and Clevers, 2016; Simian and Bissell, 2017).

However, current 3D tumor models are still quite far from recapitulating the whole *in vivo* scenario, since they do not resemble the fluid-dynamic stimuli at the cancer microenvironment level, and, consequently, the drug transport mechanisms across the vascular endothelium structure. Recently, micro-fluidic systems (so called lab-on-chip) have been developed with the ambition to overcome some of these disadvantages (Trujillo-de Santiago et al., 2019). They enable easy manipulation of liquid with microliter volumes, the generation of fluid flow induced forces and dynamic control of tumor-ECM interaction. However, in most of the cases, the fluid flow is not regulated by a peristaltic or syringe pump but guided by gravity-driven flows, thus limiting the possibility to tune and set the desired fluidic parameters (velocity, shear stress) within the circuit. Moreover, the small dimensions of these devices limit preclinical studies, since the small cell number used (typically < 1000) poorly resembles the phenotypic and cellular heterogeneity as well as microenvironmental features (Shin et al., 2012).

Moreover, the solid tumor microenvironment is highly complex and its over-miniaturization is problematic. The 3D extracellular matrix and the blood vessel walls represent physical barriers for drug transport, which determine the kinetics of drug delivery. In fact, many anticancer drugs that reach the clinic are potent enough to kill cancer cells in petri dishes (2D culture) but fail in clinical trials since they are not able to reach cancer cells in an amount that is sufficient to kill them without causing severe side effects (Das et al., 2015; Marrella et al., 2019). Therefore, a reliable *in vitro* culture system should emulate the drugs' systemic administration and their route through the vascular system to reach the tumor and penetrate to kill cancer cells.

To this aim, we here show a successful combination use of 3D cell-laden hydrogel and a fluidic culture system that more closely mimics the *in vivo* drug administration via the systemic circulation and the drug transport mechanisms across the vascular wall to the ovarian tumor mass. In detail, 3D cancer cell-laden hydrogels as ovarian cancer models (OCM) were cultured within a fluid-dynamic Multi *In vitro* Organ-MIVO® device in comparison to static conditions; as a proof-of-principle, drug efficacy of cisplatin on cell proliferation was assessed in comparison to its efficacy in a xenograft mouse model. This system may represent a

suitable *in vitro* tool to predict the efficacy of anticancer drugs and favor their clinical translation.

2 Animals, materials and methods

3D ovarian cancer model

The human ovarian cancer SKOV-3 cell line (ATCC, Manassas, VA, USA) was maintained in Dulbecco's modified Eagle's medium high glucose (HyClone – vWr) supplemented with 10% heat-inactivated fetal bovine serum (FBS), 2mM L-glutamine (Sigma Aldrich) and 1% penicillin/streptomycin solution (Sigma Aldrich) and plated at a density of $1x10^5$ cells/cm^2. The cells were incubated in a humidified, 5% CO_2 atmosphere at 37°C. Medium was changed 2 days (d) after the original plating and then twice a week. When culture dishes were nearly confluent, cells were detached with trypsin (EuroClone) after 2 washes in Dulbecco's phosphate-buffered saline (D-PBS) and replated until the next confluence. Cells were used for the *in vitro* and *in vivo* experiments after 2 passages.

Alginate (Alg) powder (Manugel GMB, FMC Biopolymer) was dissolved in physiologic solution (0.9% NaCl solution) at 1% w/v, and the solution was then filtered under sterile conditions. SKOV-3 were detached from plastic tissue culture flasks with 0.05% trypsin and resuspended in DMEM supplemented with 10% FBS and 1% penicillin/streptomycin. The SKOV-3 suspension then was mixed with the sterile Alg solution to obtain a final Alg concentration of 0.5% w/v. The SKOV-3/Alg suspension was dripped into a sterile 0.5 M $CaCl_2$ (Sigma Aldrich) gelling bath to form alginate spheres with a final concentration of cells of 1.3×10^6 cells/mL.

After washing the spheres with DI water to remove the excess calcium, the OCM were gently moved into 6 well-plates and cultured with 4.5 mL DMEM supplemented with 10% FBS, 1% penicillin/streptomycin and $CaCl_2$ (5 mM) in a humidified environment (5% CO_2) at 37°C.

Ovarian cancer model viability and proliferation

SKOV-3 viability within OCM was evaluated qualitatively through a live/dead assay (Sigma Aldrich). Briefly, after 24 h, OCM were washed with PBS and incubated in 2 mM calcein-AM and 4 mM EthD-1 in PBS for 15 min at 37°C in a dark environment to detect live and dead cells, respectively. OCM were washed 3 times in PBS and then observed by means of fluorescence microscopy (Nikon H550L).

SKOV-3 proliferation within tumor models was quantitatively assessed by Alamar Blue assay (Thermo Fisher Scientific). SKOV-3 cultured in monolayers were used as 2D control. 15×10^3 cells were cultured over a glass slide placed in a 6-well plate with the same volume of medium as the 3D models (4.5 mL). After 3 h (T0), 2 (T2), 4 (T4), or 7 d (T7) of culture, the OCM were placed in 96 well-plates containing 0.2 mL of 1% v/v Alamar Blue solution for 3D proliferation rate analysis. Samples were incubated at 37°C for 4 h in the dark. The supernatants were collected and absorbance measured spectrophotometrically. A calibration curve was derived by seeding a known number of cells in 96-well plates to find the correspondence between the number of cells and the absorbance readings. The proliferation rate was calculated as the ratio of the number of cells detected at each time point and the number of cells after 3 h of culture (T0). Then, OCM were washed with physiologic solution and placed in 6-well plates containing the original culture medium (N = 3 biological replicates; n = 2 technical replicates).

In vitro *drug efficacy tests*

A compartmental fluidic device (commercialized as MIVO® by React4life S.r.l., IT) was used to perform *in vitro* drug efficacy tests. The system design is shown schematically in Figure 1.

24-well Transwell inserts (Corning) containing one OCM each were placed and cultured within the bioreactor, forming two fluidically independent chambers: the tissue culture chamber, which was filled with culture medium (0.3 mL), and the circulatory chamber, connected to a closed loop fluidic circuit containing 4.2 mL medium circulating at a rate of 0.3 cm/s, simulating the capillary flow rate. 4 h after their formation, OCM were placed into the bioreactor chamber, and cisplatin (Sigma Aldrich srl.) was added into the bioreactor circuit connected with the receiver chamber (Fig. 1). 3D hydrogels cultured in 6-well plates with 4.5 mL medium with or without cisplatin were used as static controls.

Cell viability of cisplatin-treated SKOV-3 was assessed quantitatively by Alamar Blue assay at different time points. Briefly, the samples were placed in 96-well plates and incubated with fresh medium containing 0.2 mL of 1% v/v Alamar Blue solution at 37°C for 4 h in the dark. Cell viability was derived as % of live cells normalized to the untreated controls. Student's paired t-test between each dynamic condition and the respective static one was performed for each time point; statistical significance was set at $*P < 0.05$ (N = 3 biological replicates; n = 2 technical replicates).

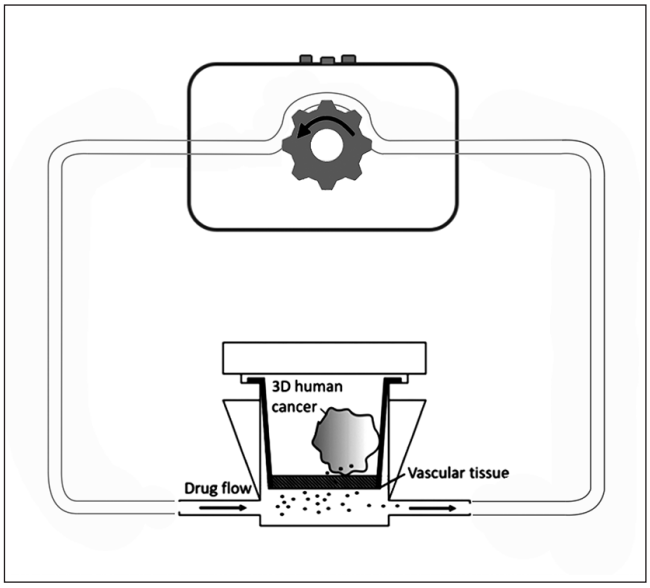

Fig. 1: Scheme of the *in vitro* 3D human cancer culture in MIVO® chamber under fluid-dynamic conditions

In vivo *xenograft model*

The study was carried out according to the guidelines enforced in Italy and in compliance with the Guide for the Care and Use of Laboratory Animals, 8th Edition, 2011. The *in vivo* experiments were authorized by the Ministry of Health for *in vivo* studies and by the Body for the Protection of Animals (OPBA).

A total of twelve 5-week-old female nude mice (Mice Hsd: Athymic Nude Foxn 1 nu female) were purchased from Envigo RMS srl, San Pietro al Natisone, Italy. The mice had a body weight of 21.1/ 20.1-24.3 g (median/interquartile range) at the beginning of the experiment. Animals were delivered to the animal facility 10 d prior to the beginning of the study for acclimatization. The mice were housed in Sealsafe Plus GM500 plastic cages (Tecniplast Spa, Buguggiate, Italy) with a light/dark cycle of 12 h/12 h at a temperature of 21 ± 2°C (dawn: 6:30-7:00 am) and a relative humidity of 60 ± 20%. Food (pellets, 10 mm, 2018 Envigo RMS Srl, San Pietro al Natisone, Italy) and sterilized water were provided *ad libitum*. A Mouse House (Tecniplast Spa, Buguggiate, Italy) was supplied as enrichment. The animals in each group were divided into 3 animals per cage. Cages were clearly labelled with an ID card indicating study number, group, gender and treatment schedule. All animals were subjected to the same environmental conditions.

SKOV-3 derived tumors were established via subcutaneous injection of 1 x 10^6 cells into the right flank of mice. The cells were resuspended in PBS for s.c. injection. Tumor size was monitored over time. After 10 d, when tumor volumes had increased to 50 mm^3, mice were randomized into 2 treatment groups, i.e., a control group (sham treated, N = 6) and an experimental group (treated, N = 6). The mice were administered PBS (control group) or cisplatin (6 mg/kg) intravenously once every 7 days for 3 weeks. Tumor growth was quantified 3 times a week using a digital caliper. The tumor volume was calculated as follows: 0.5 x length x $width^2$.

The results are expressed as tumor growth inhibition (%TGI), which was calculated as the percentage of reduction of tumor volume compared to the control:

$$\%TGI = 100 * \left(1 - \frac{TumorVolume_{treated}}{TumorVolume_{control}}\right)$$

For comparison with the *in vitro* cell viability data, the reciprocal trendline %TGI values (100-%TGI) were used.

The effect size f and total sample size were calculated using the G*Power software. The input data for the analysis were extrapolated from the published literature (Faul et al., 2007).

Immunostaining

Hydrogels were fixed with 4% paraformaldehyde in PBS (PFA; pH 7.4) for 1 h and incubated for 1 h in blocking buffer (0.5% Triton X-100, BSA 2% w/v, $CaCl_2$ 5 mM in physiologic saline solution). Subsequently, hydrogels were incubated with primary antibody for 1 h at RT. Cell proliferation was detected by staining cells with a rabbit anti-Ki67 antibody (Abcam, USA; 1:400 dilution in blocking buffer); apoptotic cells were stained by using rabbit anti-cleaved caspase-3 antibody (Abcam, USA; 1:100 dilution in blocking buffer). Samples were then washed 3 times with PBS and incubated for 1 h with Alexa Fluor 488-conjugated goat anti-rabbit secondary antibody (Abcam, USA; 1:200 dilution in blocking buffer) for anti-Ki67 and with Alexa Fluor 555-conjugated goat anti-rabbit secondary antibody (Abcam, USA; 1:200 dilution in blocking buffer) for anti-caspase-3. Nuclei were counter-labeled with DAPI (Sigma-Aldrich). Imaging was performed with a fluorescence microscope (Nikon H550L). Images obtained by fluorescence microscopy were analyzed using ImageJ software.

Drug diffusion within the 3D tumor hydrogel

Drug diffusion into the 3D tumor hydrogel was determined via HPLC. Alginate hydrogels were cultured either under static conditions or within the MIVO® for 7 d with 10 µM cisplatin. The hydrogels were then left in the incubator for 3 d in 5 mM $CaCl_2$ physiologic solution to allow the cisplatin to diffuse from the hydrogel to the solution. Then the samples were analyzed by HPLC. The HPLC system consisted of a pump, column compartment and RS variable wavelength detector (all UltiMate 3000, Thermo Fisher Scientific). The injection valve fitted with a 20 µL sample loop and an Accucore 150-C18 (Dimensions = 150 x 3 cm and particle size 2.6 µm) was purchased from Thermo Fisher Scientific. The mobile phase consisted of methanol-water (80:20, v/v). The UV detector was adjusted to 254 nm. The flow rate was set at 0.2 mL/min (isocratic flux) and the column temperature at 40°C (Kaushik et al., 2010; Tezcan et al., 2013) (N = 3 biological replicates).

Computational fluid-dynamic (CFD) simulations

Fluid dynamic and mass transport simulations were performed both in static and dynamic conditions to simulate the concentration of cisplatin within the cell-laden hydrogels over time.

The 3D domain, the related size and dimensions were calculated based on the dimensions of the microfluidic circuit used during the test. As shown in Figure S1[1], Domain 1 represents the circulatory chamber of the bioreactor and the fluidic pattern of the circuit, Domain 2 is the tissue culture chamber, which is represented by a well filled with medium, and Domain 3 represents the alginate-based hydrogel sphere. The obtained geometry, the fluid dynamics within the circuit, and the mass transport of cisplatin through the entire system was modeled using Comsol Multiphysics 5.3a. For the numerical solution of the physics involved in this system, the *Laminar Fluid Flow module* and the *Transport of Diluted Species module* were used.

The first physical phenomenon involved in this system was represented by the fluid dynamics from the circulatory chamber of the bioreactor (Domain 1) to the tissue culture chamber (Domain 2) where the cell-laden hydrogel is cultured (Domain 3). The fluid was supposed to be laminar, incompressible, and

[1] doi:10.14573/altex.2003131s

not turbulent. The velocity and pressure field profiles were calculated according to Navier-Stokes and the continuity equation (Equation 1):

$$\begin{cases} \rho(u \cdot \nabla u) = -\nabla p + \mu \nabla^2 u \\ \rho(\nabla \cdot u) = 0 \end{cases} \quad \text{(Equation 1)}$$

where u, ρ and μ are the velocity, the density (10^3 kg/m^3) and the viscosity (10^{-3} $Pa{\cdot}s$) of the fluid, respectively, and p is the pressure. The flow rate was set to Q=3 mL/min to generate velocity resembling the capillary blood flow. An iterative geometric multigrid (GMRES) algorithm was used to solve the equations. Discretization was chosen P2 + P1 for velocity and pressure field, respectively. In the outlet, the pressure was set equal to zero with no backflow. A no-slip condition was fixed on the boundary of the geometry. As the initial value, the velocity was set equal to zero in the entire system.

The general mass transport equation was used to describe cisplatin mass transport through the system:

$$\frac{\partial c}{\partial t} + \nabla(-D\nabla c) + u\nabla c = R \quad \text{(Equation 2)}$$

where c is the cisplatin concentration in the system, D is the diffusivity of cisplatin, u is the velocity field, and R is the reaction term. The diffusivity of cisplatin D in the medium (approximated as water) at 37°C ($D_w^{Cis\text{-}Pt}$), included in the equation for Domains 1 and 2, is set equal to $1.034 * 10^{-5} cm^2/s$, as reported in the literature (Modok et al., 2007; Panczyk et al., 2013).

The diffusion constant of cisplatin within the alginate hydrogels ($D_{hy}^{Cis\text{-}Pt}$) was calculated by using the empirical Ogston model, as shown in Equation 3. The model takes into account several parameters including the polymer volume fraction ϕ, the solute (cisplatin) radius r_s, the alginate fiber radius r_f, and the diffusion value of cisplatin in water $D_w^{Cis\text{-}Pt}$. In particular, the value was calculated using the following expression:

$$\frac{D_{hy}^{Cis-Pt}}{D_w^{Cis-Pt}} = \exp\left(-\frac{r_s + r_f}{r_f}\phi^{0.5}\right) \quad \text{(Equation 3)}$$

where the polymer volume fraction was approximated to 0.01, while the radius of cisplatin and alginate fiber were $4 \cdot 10^{-10} m$ and $8 \cdot 10^{-10} m$, respectively (Amsden, 1998; Modok et al., 2007).

Moreover, it should be considered that the diffusivity value of cisplatin in the alginate hydrogels is affected by the presence of dead cells, which decrease the mass transport of cisplatin within the polymer.

Firstly, the Michaelis-Menten parameters were calculated by considering that 50,000 molecules of cisplatin are enough to kill one cell (Amsden, 1998), as reported in the following reaction (Equation 4):

$$50{,}000\ molecules\ of\ cisplatin + 1\ cell \rightarrow 1\ dead\ cell \quad \text{(Equation 4)}$$

Based on the best fitting of the experimental data (Fig. S3[1]), the obtained values were V_{max}=1.66 · 10^{-12} [$mol * m^{-3} * s^{-1}$] and K_m= 6.64 · 10^{-3} [$mol * m^{-3}$].

In this case, the Ogston model considers an added corrective term to describe the mass transport in the system. Therefore, the diffusion of cisplatin within the hydrogel could be described by the following equation:

$$D_{hy}^{Cis-Pt} = D_w^{Cis-Pt} \cdot a \cdot \exp\left[\frac{-k \cdot t}{t+b}\right] \quad \text{(Equation 5)}$$

where $D_w^{Cis\text{-}Pt}$ is the diffusivity of cisplatin in water, a is the ratio calculated according to the Ogston model (equal to 0.86 in Equation 3), and the exponential term defines the decrease of the diffusion during the time t due to the presence of dead cells.

Parameters k and b (Tab. 1) depend on the velocity field (either in static or dynamic conditions) and were calculated considering the amount of cisplatin within the alginate hydrogels experimentally measured through HPLC analysis after 7 d of culture.

The initial concentration of cisplatin (C_0) in the bioreactor was set at 100 µM or 10 µM.

Danckwerts conditions were selected in the inlet, while in correspondence of the boundary surfaces no-flux condition was considered. For the outlet, the diffusion term was considered equal to zero.

A direct backward differentiation formula (BDF) algorithm was required for the transient study. Linear discretization was chosen for the concentration field. The reaction term was defined according to the Michaelis-Menten kinetics:

$$R = -\frac{V_{max} \cdot c}{K_m + c} \quad \text{(Equation 6)}$$

where V_{max} is the maximum consumption rate and K_m is the concentration of cisplatin when the rate is equal to $V_{max}/2$. The reaction term takes into account the deactivation of cisplatin molecules bound to the DNA of cancer cells and no longer available during the experimental tests. This term was considered as a consumption rate of cisplatin.

The average concentration profile of cisplatin within the hydrogels was calculated as follows:

$$C = \frac{1}{V_{sphere}} \int_{sphere} C(x, y, z) dV \quad \text{(Equation 7)}$$

Tab. 1: Values for the cisplatin diffusivity in static and dynamic conditions

	Static	Dynamic
k	9.5 ± 0.05	6 ± 0.05
b(s)	4x10^3 ± 100	4x10^3 ± 100

3 Results

3.1 3D cancer cell viability and proliferation

Firstly, ovarian cancer cell viability and growth within the OCM were investigated and visualized by calcein-AM staining. Most of the cells were alive 4 h after OCM generation (Day 0), indicating the suitability of the procedure for cellular embedment within the alginate hydrogels. Cell viability was evaluated also after 7 days

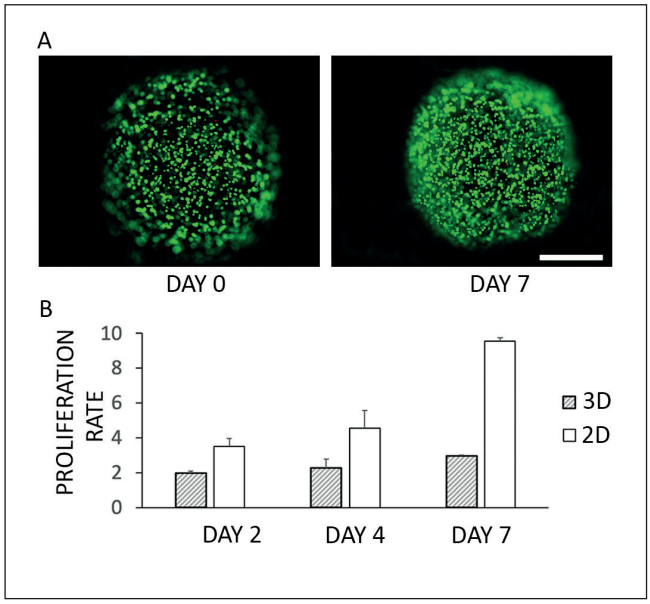

Fig. 2: Cell viability and proliferation of OCM in culture
(A) Cell viability represented by live/dead images of OCM after 4 hours (Day 0) and 7 days (Day 7) of culture. Scale bar is 500 μm. (B) Quantitative analysis of the proliferation rate of ovarian cancer cells embedded within alginate hydrogels (3D) or cultured in monolayers (2D) assessed by Alamar Blue assay. Values are reported as mean ± SD. (N = 3 biological replicates; n = 2 technical replicates).

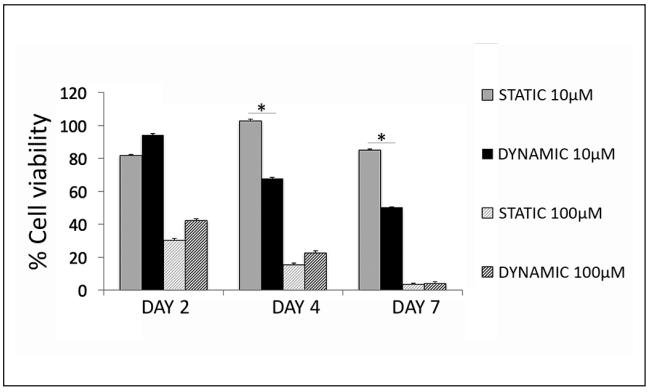

Fig. 3: Cell viability of SKOV-3 culture assessed by Alamar Blue assay within OCM in static and in dynamic conditions treated with the indicated concentration of cisplatin
Cell viability was derived as % of live cells normalized to the untreated controls. Values are reported as mean ± SD. Student's paired t-test between each experimental dynamic condition and the respective static one for each time point was performed and statistical significance was set at *, $P < 0.05$ (N = 3 biological replicates; n = 2 technical replicates).

of culture. A higher cell density was observed at Day 7, proving the cells' ability to proliferate within the hydrogel (Fig. 2A).

To quantify this result, the cell proliferation rate was measured by Alamar Blue assay after 2, 4 and 7 days of culture. Figure 2B shows that cancer cells cultured within the OCM proliferate more slowly than cells grown in 2D monolayers, which is in agreement with other reports (Chitcholtan et al., 2013).

3.2 *In vitro* drug efficacy test

The viability of SKOV-3 OCM cultured in MIVO® and treated with cisplatin (10 µM or 100 µM) was measured over time. In particular, while in static conditions the drug was directly added to the medium surrounding the OCM, in dynamic conditions (i.e., MIVO®) it was injected into the fluidic circuit beneath the membrane from which it could reach the tumor tissue cultured in the upper chamber of the bioreactor by diffusion, resembling extravasation of the drug.

After two days of culture in the presence of 100 µM cisplatin, cell viability in static and in dynamic conditions was significantly reduced and was even lower after 4 and 7 days, with no significant differences observed between static and dynamic conditions (Fig. 3).

Viability was weakly but not significantly reduced after two days culture in the presence of 10 µM cisplatin under static conditions. Interestingly, significantly decreased cell viability to 67.81% ± 0.62 and 50.44% ± 0.25 after 4 and 7 days, respectively, at 10 µM cisplatin was observed only under dynamic conditions in MIVO®. OCM cultured under static conditions remained above 80% cell viability for the overall time of observation (Fig. 3).

3.3 *In vivo* drug efficacy test

The *in vivo* efficacy of cisplatin against SKOV-3 cells was evaluated in a xenograft model. Treatment of six nude mice with 6 mg/kg cisplatin versus six control mice started 10 days after tumor induction, defined as Day 0. The experiment was stopped on Day 35 when the tumor volume in the control group reached 2000 ± 270 mm^3 and was more than double compared to the treated group (see Fig. S2[1] for tumor volume data). Figure 4A shows the inhibitory effect of cisplatin on tumor growth over time.

The %TGI was 7.3%, 31.1% and 56.9% on Days 12, 21 and 35, respectively, as shown in Figure 4A. Interestingly, comparing the endpoints of the *in vitro* (static treatment), in MIVO® (dynamic treatment) and *in vivo* (xenograft model) efficacy tests, an excellent overlap of drug efficacy data was observed only between MIVO® and *in vivo* data, although on a different time scale (Fig. 4B); comparable results were obtained after 2,4 and 7 days of treatment in MIVO® and after 2, 11 and 25 days of treatment in mice. Due to the differences in drug distribution and metabolism (ADME profiles) between these two different experimental conditions, the time needs to be rescaled to obtain comparable results (~3 times faster in MIVO®). Static *in vitro* results did not resemble data obtained *in vivo*.

3.4 CFD simulations and mass transport in MIVO®

The concentration fields of 10 µM cisplatin within the OCM cultured in static and dynamic conditions are shown in Figure 6 based on the geometry and the model set-up defined in Section 2.

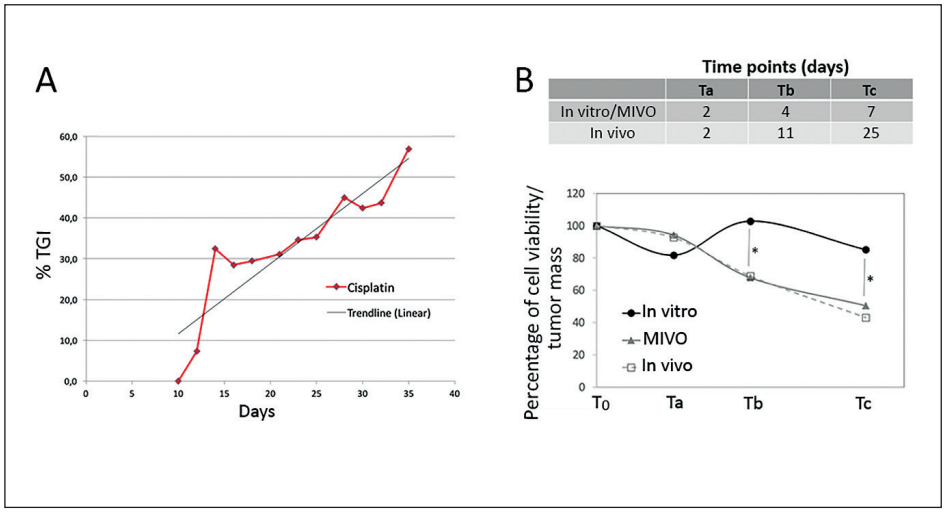

Fig. 4: Tumor regression in the xenograft model and comparison with *in vitro* and MIVO®
Panel A: Tumor regression in the xenograft model after 6 mg/kg cisplatin treatment in comparison with the control (sham-treated animals, N = 6). Values are reported as mean of tumor growth inhibition (%TGI). Panel B: Comparison of *in vitro* (static condition), MIVO® (dynamic condition) and *in vivo* data. For *in vitro* data, 10 μM cisplatin data from Figure 3 was used. Values are reported as mean ± SD. One-way Anova. *, $P < 0.05$.

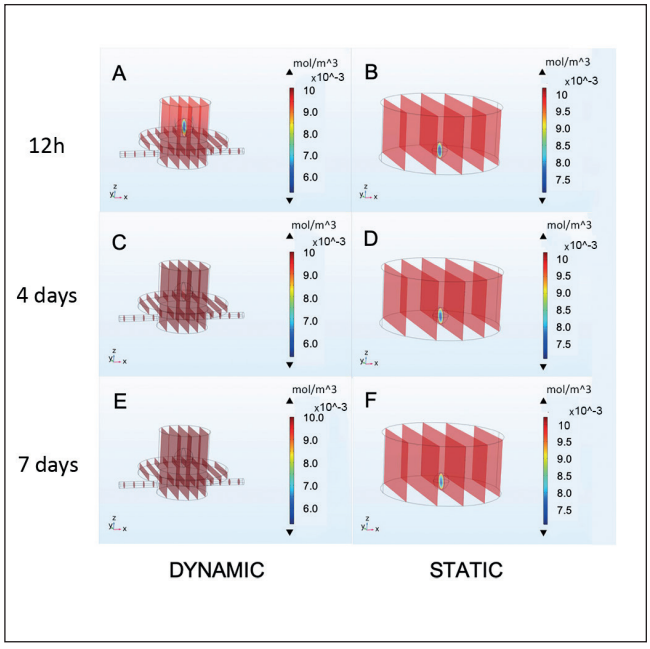

Fig. 5: Distribution of cisplatin in dynamic and static conditions at 10 μM and different time points
(A) dynamic; 12 h, (B) static; 12 h, (C) dynamic; 4 days, (D) static; 4 days, (E) dynamic; 7 days, (F) static; 7 days. While the dynamic condition shows a complete drug distribution within the 3D volume after 7 days of culture, a strong gradient is still present under static conditions.

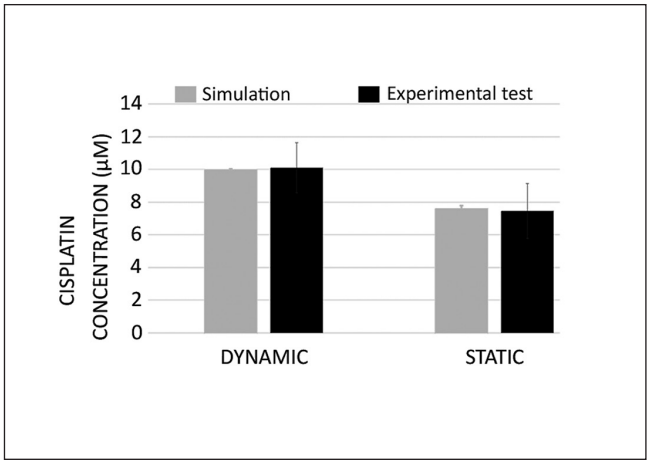

Fig. 6: Concentration of cisplatin in OCM after 7 days culture in dynamic or static conditions
Comparison between the amount estimated by simulation and measured by HPLC in the tests. Cisplatin concentration: 10 μM. Values are reported as mean ± SD (N = 3 biological replicates).

After 12 hours, the amount of cisplatin diffused within the alginate spheres seemed to be higher in the static than in the dynamic condition, i.e., values of 0.0053 mol/m^3 and 0.00707 mol/m^3 were detected for the dynamic and the static conditions, respectively (Fig. 5A,B). Interestingly, after 4 days of culture, the trend was opposite, with higher amounts of cisplatin in dynamic than in static conditions (Fig. 5C,D). The same results were also obtained after 7 days. Specifically, in the dynamic culture, the alginate hydrogel was completely filled with cisplatin, while in static conditions concentration gradients through the sphere were still evident (Fig. 5E,F).

Simulations were performed at the two concentrations tested *in vitro* (10 µM and 100 µM). No major differences between the amount of cisplatin simulated in the model and that measured experimentally were detected (Fig. 6), illustrating the reliability of the mathematical model.

The average concentration profiles of cisplatin within the hydrogels showed a significant difference among the different cases tested over 7 days, as shown in Figure 7. The diffusion of the drug within the hydrogels in static conditions was faster at short time scales at both concentrations (100 µM and 10 µM) than in dynamic conditions. It is likely that when the hydrogel placed in the well plate was dipped in the cisplatin solution, the concentra-

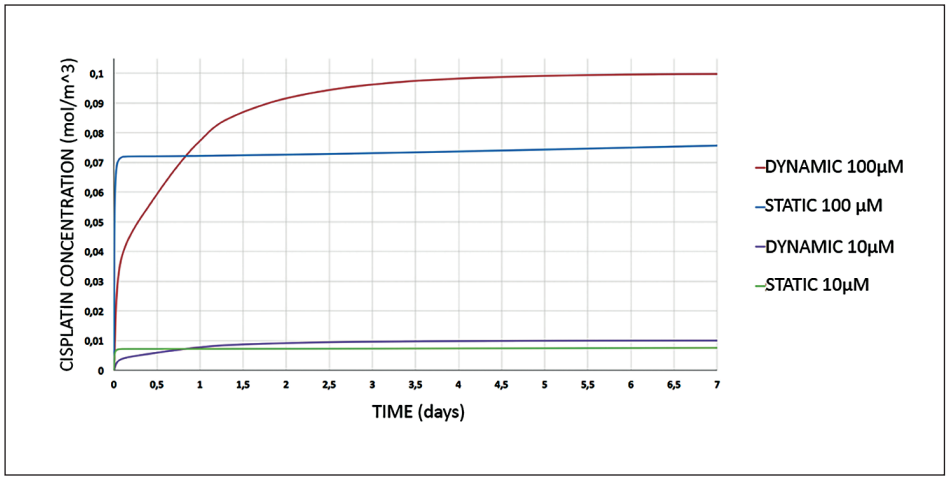

Fig. 7: Concentration profile of cisplatin in OCM over time for the four different experimental conditions
For each drug concentration (10 or 100 μM), the dynamic condition shows a slower diffusion over time that reaches a higher plateau value.

tion gradients of the drug were high enough to allow a fast diffusion through the hydrogel. It should be noted that the corresponding convection term is missing in static conditions.

In dynamic conditions, the cisplatin concentration within the hydrogels increased slowly and reached the same concentration as in the static condition after 18 hours, both at 100 and 10 µM. Under these conditions, the drug needed to move from Domain 1 to Domain 2, finally reaching Domain 3 (Fig. S1[1]). However, the concentration of cisplatin within the hydrogels became higher than in static conditions after one day of culture. After 4 days of culture in dynamic conditions, the cisplatin concentration reached a plateau, and a clear difference in cisplatin concentration between the two culture conditions was detected at both tested concentrations (i.e., 100 and 10 µM), as shown in Figure 7.

In summary, in static conditions, the absence of fluid motion generates a greater cisplatin resistance within the hydrogel due to the accumulation of dead cells, which limit the mass transport within the polymer. In contrast, in dynamic conditions, the flow allows continuous removal of dead cells, thus leading to less hydrogel resistance to cisplatin diffusion.

3.5 Immunostaining

Immunostaining of OCM collected at different time points was carried out to determine the expression of Ki67 to identify proliferating cells and of caspase-3 to mark cells undergoing apoptosis in response to treatment with cisplatin (Fig. 8 and Fig. S4[1], respectively).

Ki67-positive cells were detected in untreated OCM cultured in static (Fig. 8, Fig. S4[1]) or dynamic conditions (Fig. S5A[1]) after 2 days of culture, and numbers increased further after 7 days.

Interestingly, cell-laden hydrogels treated with 10 µM cisplatin under dynamic conditions displayed an overall positive staining for proliferating cells comparable to untreated hydrogels after 2 days, however the Ki67 staining was drastically reduced after 7 days (Fig. 8A). This behavior was even more evident for the high dose of the drug (i.e., 100 µM) (Fig. S4[1]).

When the tumor tissue was treated under static conditions, there was less Ki67 staining than in untreated hydrogels or un-

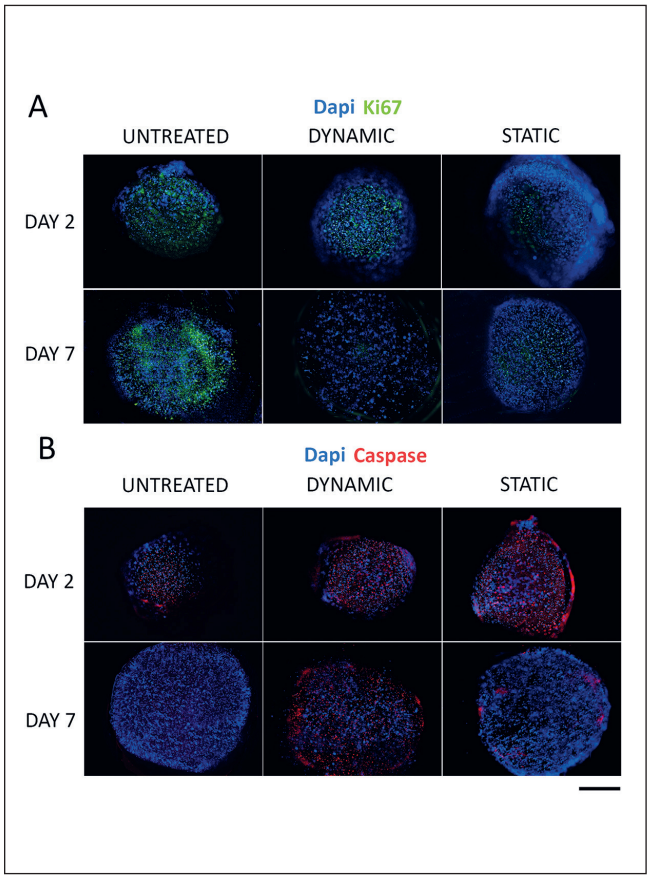

Fig. 8: Fluorescence images showing immunostaining of Ki67 (green) as marker of proliferation and caspase-3 (red) as marker of apoptosis of SKOV-3 cultured within alginate hydrogels treated with 10 μM cisplatin in static or dynamic conditions (MIVO®)
The untreated controls were cultured in static conditions. Cells were stained after 2 or 7 days and counter-labeled with DAPI (blue). Scale bar is 500 μm (N = 3 biological replicates; n = 2 technical replicates).

der dynamic conditions after 2 days, and Ki67 staining was still well evident after 7 days of 10 µM drug treatment, especially in the inner part of the hydrogel (Fig. 8A). When the treatment was carried out at the higher drug concentration, Ki67 staining was reduced compared to the 10 µM dose (Fig. S4[1]).

These data are in line with the cell viability reduction shown in Figure 3.

The expression of caspase-3 was weak in the untreated control after 2 days and almost undetectable after 7 days in static and dynamic conditions (Fig. 8, Fig. S4[1], Fig. S5A[1]). Positive caspase staining was observed in both static and dynamic conditions after 2 days of 10 µM drug treatment (Fig. 8B); this was much more evident for samples treated with 100 µM (Fig. S4[1]); interestingly, after 7 days of treatment in the MIVO® device, cell-laden hydrogels displayed a homogeneous spatial distribution of apoptotic cells, while samples treated in static conditions displayed caspase-positive staining mainly in the outer rim of the OCM, indicating an accumulation of dead cells that could form a physical barrier hindering cisplatin diffusion (Fig. 8B). Again, this was much more evident for samples treated with 100 µM (Fig. S4[1]).

4 Discussion

The ability to rapidly and efficiently screen drugs with a more accurate preclinical tumor model is of great importance in drug development, because currently used assays still have severe limitations and poor predictivity. Considering the limitations of animal experiments to predict human response and the high need for novel drugs, it is necessary to include highly reproducible human systemic tumor models in preclinical analyses to validate the efficiency of drug candidates more accurately.

Recently, regulatory authorities have voiced a common desire to standardize the preclinical tests of drugs by replacing/reducing animal experimentation during early product development with specific *in vitro* systems, summarized in Table 2 (Daniel et al., 2018). This can be achieved only by strictly linking academic research outcomes with key industry entities to foster the implementation and optimization of relevant *in vitro* models on a large scale. The production of scientific data supporting the high reliability of alternative animal models is the first step to support industries in reducing time and costs of preclinical research.

In our previous work, a fluidic device was adopted to culture a breast cancer tumor model *in vitro*, resembling some crucial steps of tumor growth: cell migration within the 3D hydrogel, cell evasion from the hydrogel, and intravasation into the fluid circuit (Cavo et al., 2018). Likewise, oral administration and the subsequent intestinal passage of other kinds of molecules and drugs can be modeled with the MIVO® chamber, as already reported (Marrella et al., 2020). Starting from these promising results, we have here combined the use of a 3D cell-laden hydrogel as an ovarian tumor model of clinically relevant size with the MIVO® fluidic device to resemble the human circulation and drug extravasation to reach the tumor mass. To test this technological approach, a drug efficacy assay was carried out as a proof-of-principle in parallel to a xenograft model, which represents the current gold standard. For comparison, the 3D tumor models were also cultured under static conditions, resembling the traditional assays using organoids/spheroids.

In order to further decrease the use of animals in pre-clinical research, serum-free medium can be a valuable option to perform *in vitro* cell culture. Along this line, also the use of recombinant antibodies rather than animal-derived ones can be desirable. In this work, FBS and animal-derived antibodies were used to validate this novel technological approach by comparing the results with data present in the literature and internal to our laboratory practice. In the near future we will move towards the evaluation of the use of alternative animal-free strategies for cellular assays, in accordance with the 3R principles.

Here, the ovarian tumor was selected since it has the highest mortality rate of all gynecological cancers worldwide (Siegel et al., 2012). However, this approach can be extended to many other solid tumors. SKOV-3 were embedded within 3D hydrogels or injected into mice, as previously reported (Cavo et al., 2018; Marrella et al., 2019).

The tumor model is composed of a cell-laden hydrogel. Among polymers, alginate was selected for its well-known advantages like inertness, chemical stability, and lack of intrinsic bioactivity (Khurana and Godugu, 2018) to better focus on the drug penetration mechanisms and compare the *in vitro* model with the scaffold-free xenograft model. Further experiments could investigate increasing the level of complexity of the tissue model by combining different biopolymers and by incorporating multiple cell types associated with the ovarian tumor niche (e.g., fibroblasts, myofibroblasts, pericytes, vascular or lymphatic endothelial cells, and undifferentiated mesenchymal stem cells) to better model the tumor microenvironment, which is a complex, heterogeneous and multi-cellular environment involving dynamic interactions between malignant cells and their surrounding stroma, including both cellular and acellular components.

Cisplatin was selected since it represents, together with its analogs, the first-line chemotherapeutic agent for the treatment of human ovarian cancer, exerting its cytotoxicity by forming DNA-links, which trigger apoptosis (Tiwari et al., 2005). The drug concentration tested *in vivo* (6 mg/kg) was adopted because it represents the "maximum tolerated dose", i.e., the most efficient dose without toxic effect (Aston et al., 2017). Two concentrations were employed *in vitro* to investigate a concentration-dependent cytotoxic effect and also to enable a comparison with *in vivo* data. For the higher drug concentration tested (100 µM), we observed that most of the cells died after a few days of culture, both in the static and the dynamic conditions, indicating excessive toxicity. Differently, with the lower drug concentration (10 µM), the decrease in tumor cell proliferation was greater in the dynamic than in the static condition. Moreover, this drug concentration, which is commonly used to perform *in vitro* drug efficacy tests (Gao et al., 2015; Tang et al., 2015), induced cytotoxic effects of the drug over one week that were comparable with those observed *in vivo* over three weeks.

It is an important aspect to determine at what concentration and for what duration a drug should be administered *in vitro* to

Tab. 2: Main advantages and limitations of the different tumor models available for drug tests

Model	Main advantages	Main limitations
2D culture	– easy to culture – cheap – reproducible	– aberrant cell proliferation – limited cell-cell and cell-ECM interactions – oversimplified
3D scaffold-free spheroid	– cheap – no scaffold-associated batch-to-batch variations – possibility to co-culture different cell types	– susceptible to physical disintegration – lack of surrounding ECM
3D matrix-assisted tumor model	– mimic the ECM – cell-cell and cell-matrix interactions in all spatial directions – tunable stiffness and ECM chemical composition	– lack of fluid-dynamic stimuli typical of the tumor environment – unreliable drug diffusion and drug transport mechanisms
3D fluid-dynamic tissue culture (e.g., MIVO® device)	– resembling the tumor fluid-dynamic environment – resembling the drug systemic administration – reduction of the time of drug testing outcome compared to *in vivo* assays	– hard to mimic drug distribution among organs and metabolism (ADME profiles) – reduced tissue-tissue and organ-organ connection
***In vivo* model**	– high tissue complexity – high degree of realism	– expensive – time-consuming – different metastatic progression if compared to human case – ethical concerns

allow an *in vitro-in vivo* comparison so that the use of animal models in the preclinical phase can be reduced in future.

The MIVO® platform allows to drastically reduce the overall experimental time, since there is no need to wait for the tumor tissue to grow in mice after cancer cell injection. Moreover, the platform can cut out two highly time-consuming stages of pre-clinical trials: the complex bureaucratic procedure for obtaining ethical clearance, which can take 3-6 months to be completed, and the quarantine, stabilization and acclimation of the mice, which requires around 1 month on average, reaching a total of up to 7 months to prepare a single experiment. The MIVO®-based approach allows the reduction of these times to a couple of weeks of experimental tests, thus potentially reducing the release time of new medicines, animal use and expenditure.

Interestingly, previous studies reported a higher resistance to chemotherapy of 3D tumor models when compared to traditional 2D assays (Talukdar and Kundu, 2012; Stock et al., 2016; Lhuissier et al., 2017; Curtin et al., 2018). This is confirmed by our data shown in Figure S6[1], where SKOV-3 cultured in 2D conditions were treated with the same cisplatin concentration used in the 3D tumor models (i.e., 10 µM). Already after 2 days of culture, the viability was reduced to about 40% in 2D in comparison to 80% found for the 3D culture (Fig. 2). These results confirm that monolayer-based assays overestimate the drug-cell interactions and the drug diffusion due to a lack of ECM.

To our knowledge this is the first time a drug-induced *in vitro* tumor regression curve is reported that is comparable to that measured in a xenograft model. This was achieved by modeling *in vitro* (i) 3D tumor tissue perfusion under a capillary circulation, and (ii) the systemic drug transport mechanisms. In contrast, the 3D tumor tissue treated under static conditions displayed resistance to the cytotoxic agent over time, in agreement with the literature. The combination of computational fluid dynamic simulation, drug diffusion measurements and immune-staining analysis allowed to demonstrate the reasons for these results, and in particular the poor reliability of static 3D tumor hydrogel culture for drug efficacy assays. In particular, when 3D tumor hydrogels were cultured in MIVO® and the drug agent was flowing within the circuit, the reduction of cell viability began later than in static conditions. This is in line with the computational modeling results (Fig. 6, 7), showing that the cisplatin diffusion within the tumor hydrogel is initially faster when the drug is added around the 3D hydrogel (in static), while the drug extravasation under flow takes more time. Interestingly, cancer cell viability decreased over time at the lower cisplatin dose only under fluid-dynamic conditions in MIVO®, displaying a continued cytotoxic effect of the drug comparable to that observed *in vivo* and in contrast to the *in vitro* static approach. We hypothesize this is due to different mechanisms of drug penetration within the OCM over time, and to a poor and unreliable drug exposure under static conditions. When the cancer cell culture is carried out under static conditions, the drug initially enters the 3D hydrogel and may produce its cytotoxic effect mainly in the external layer of cells, which then create a kind of physical barrier for the drug, limiting its continuous diffusion towards the inner core of the polymeric matrix. When, instead, the OCM are cultured in MIVO®, the fluid circulation resembling the capillary blood flow improves the mass transport

and waste removal, thus supporting continuous drug diffusion within the hydrogel. These hypotheses were proven by measuring the cisplatin diffusion within the hydrogels in static and dynamic conditions, respectively (Fig. 7).

As a further control, the 3D tumor hydrogels were cultured for 7 days in dynamic versus static conditions without cisplatin (Fig. S5B[1]). The proliferation rate of the cells was comparable, with a trend to a higher proliferation rate in dynamic conditions in comparison to static conditions. These data consolidate the results obtained, showing that the decrease of cell viability after 7 days observed in hydrogels cultured in MIVO® treated with cisplatin is due to mechanisms of drug penetration within the hydrogel provided by the fluidic stimulation, not to reduced cellular proliferation under dynamic conditions. These data are consistent with previous work, which reported that the exposure of ovarian cancer cells to low magnitude fluid shear stress (as in MIVO® chamber) can induce ovarian cancer progression (Ip et al., 2016).

This is supported by immunostaining against proliferating cells (i.e., Ki67) and apoptotic cells (i.e., caspase-3) in both tissue culture conditions (Fig. 8, Fig. S4[1]). As expected, after 7 days of drug treatment, proliferating cells were observed under static conditions in the core volume of the OCM, while very few Ki67-positive cells were found within the 3D hydrogels cultured in MIVO®. Moreover, an external barrier of apoptotic cells was stained in static conditions, while cell-laden hydrogels in MIVO® displayed a homogeneous spatial staining of caspase-3. These results were observed at both drug concentrations and were more evident at the higher concentration.

The experimental measurements of cisplatin concentration within the hydrogels through HPLC confirmed the different drug diffusion kinetics within the polymeric matrix: after 7 days of drug treatment, the drug nominal concentration (i.e., 10 μM) was found within the hydrogels that had been cultured in dynamic conditions, while a lower concentration (7 μM) was measured in the hydrogels that had been cultured under static conditions.

These results confirm the key role of the fluid-dynamic environment in resembling the physiological 3D tumor tissue mass and drug transport through a fluid-dynamic stream of the blood circulation *in vitro*. Under these conditions, obtained by using the MIVO® tissue culture device, the *in vitro* tumor regression curve resembles the tumor mass reduction measured *in vivo* though in a shorter time. In fact, the same drug efficacy results were obtained *in vitro* in just 1 week instead of 5 weeks as *in vivo*. This is mainly due to a different clearance and distribution of the drug in the two different experimental conditions. These results highlight that the *in vivo*-like dynamic environment provided by the MIVO® device allows to better resemble 3D tumor tissue perfusion and its culture under a capillary circulation and the systemic drug transport mechanisms, suggesting its potential as a relevant platform for preclinical drug efficacy tests.

In conclusion, the combination of 3D tumor models with the MIVO® fluidic device may have great potential as a novel and human-relevant preclinical drug efficacy assay. This could allow improvement of the drug development process and lead to more effective, standardized, fast and ethical *in vitro* outcomes, finally leading towards significant patients benefits.

References

Abbott, A. (2003). Biology's new dimension. *Nature 424*, 870-872. doi:10.1038/424870a

Amsden, B. (1998). Solute diffusion within hydrogels. Mechanisms and models. *Macromolecules 31*, 8382-8395. doi:10.1021/ma980765f

Aston, W. J., Hope, D. E., Nowak, A. K. et al. (2017). A systematic investigation of the maximum tolerated dose of cytotoxic chemotherapy with and without supportive care in mice. *BMC Cancer 17*, 684. doi:10.1186/s12885-017-3677-7

Brancato, V., Oliveira, J. M., Correlo, V. M. et al. (2020). Could 3D models of cancer enhance drug screening? *Biomaterials 232*, 119744. doi:10.1016/j.biomaterials.2019.119744

Burleson, K. M., Casey, R. C., Skubitz, K. M. et al. (2004). Ovarian carcinoma ascites spheroids adhere to extracellular matrix components and mesothelial cell monolayers. *Gynecol Oncol 93*, 170-181. doi:10.1016/j.ygyno.2003.12.034

Cavo, M., Caria, M., Pulsoni, I. et al. (2018). A new cell-laden 3D Alginate-Matrigel hydrogel resembles human breast cancer cell malignant morphology, spread and invasion capability observed "in vivo." *Sci Rep 8*, 5333. doi:10.1038/s41598-018-23250-4

Chitcholtan, K., Asselin, E., Parent, S. et al. (2013). Differences in growth properties of endometrial cancer in three dimensional (3D) culture and 2D cell monolayer. *Exp Cell Res 319*, 75-87. doi:10.1016/j.yexcr.2012.09.012

Clevers, H. (2016). Modeling development and disease with organoids. *Cell 165*, 1586-1597. doi:10.1016/j.cell.2016.05.082

Curtin, C., Nolan, J. C., Conlon, R. et al. (2018). A physiologically relevant 3D collagen-based scaffold-neuroblastoma cell system exhibits chemosensitivity similar to orthotopic xenograft models. *Acta Biomater 70*, 84-97. doi:10.1016/j.actbio.2018.02.004

Daniel, A. B., Strickland, J., Allen, D. et al. (2018). International regulatory requirements for skin sensitization testing. *Regul Toxicol Pharmacol 95*, 52-65. doi:10.1016/j.yrtph.2018.03.003

Das, V., Bruzzese, F., Konečný, P. et al. (2015). Pathophysiologically relevant in vitro tumor models for drug screening. *Drug Discov Today 20*, 848-855. doi:10.1016/j.drudis.2015.04.004

Dutta, R. C. and Dutta, A. K. (2009). Cell-interactive 3D-scaffold; advances and applications. *Biotechnol Adv 27*, 334-339. doi:10.1016/j.biotechadv.2009.02.002

Fang, Y. and Eglen, R. M. (2017). Three-dimensional cell cultures in drug discovery and development. *SLAS Discov 22*, 456-472. doi:10.1177/1087057117696795

Fatehullah, A., Tan, S. H. and Barker, N. (2016). Organoids as an in vitro model of human development and disease. *Nat Cell Biol 18*, 246-254. doi:10.1038/ncb3312

Faul, F., Erdfelder, E., Lang, A.-G. et al. (2007). G*Power 3: A flexible statistical power analysis program for the social, behavioral, and biomedical sciences. *Behav Res Methods 39*, 175-191. doi:10.3758/bf03193146

Gao, Y., Shan, N., Zhao, C. et al. (2015). LY2109761 enhances cisplatin antitumor activity in ovarian cancer cells. *Int J Clin Exp Pathol 8*, 4923-4932.

Herter, S., Morra, L., Schlenker, R. et al. (2017). A novel three-dimensional heterotypic spheroid model for the assessment of the activity of cancer immunotherapy agents. *Cancer Immunol Immunother 66*, 129-140. doi:10.1007/s00262-016-1927-1

Hoarau-Véchot, J., Rafii, A., Touboul, C. et al. (2018). Halfway between 2D and animal models: Are 3D cultures the ideal tool to study cancer-microenvironment interactions? *Int J Mol Sci 19*, 181. doi:10.3390/ijms19010181

Huber, J. M., Amann, A., Koeck, S. et al. (2016). Evaluation of assays for drug efficacy in a three-dimensional model of the lung. *J Cancer Res Clin Oncol 142*, 1955-1966. doi:10.1007/s00432-016-2198-0

Hutmacher, D. W., Loessner, D., Rizzi, S. et al. (2010). Can tissue engineering concepts advance tumor biology research? *Trends Biotechnol 28*, 125-133. doi:10.1016/j.tibtech.2009.12.001

Ip, C. K. M., Li, S. S., Tang, M. Y. H. et al. (2016). Stemness and chemoresistance in epithelial ovarian carcinoma cells under shear stress. *Sci Rep 6*, 26788. doi:10.1038/srep26788

Jiguet Jiglaire, C., Baeza-Kallee, N., Denicolaï, E. et al. (2014). Ex vivo cultures of glioblastoma in three-dimensional hydrogel maintain the original tumor growth behavior and are suitable for preclinical drug and radiation sensitivity screening. *Exp Cell Res 321*, 99-108. doi:10.1016/j.yexcr.2013.12.010

Kaushik, K. H., Sripuram, V. K., Bedada, S. et al. (2010). A simple and sensitive validated HPLC method for quantitative determination of cisplatin in human plasma. *Clin Res Regul Aff 27*, 1-6. doi:10.3109/10601330903490462

Khurana, A. and Godugu, C. (2018). Alginate-based three-dimensional in vitro tumor models: A better alternative to current two-dimensional cell culture models. In B. Rehm and M. Moradali (eds.), *Alginates and Their Biomedical Applications* (157-183). Springer Series in Biomaterials Science and Engineering. Volume 11. Singapore: Springer. doi:10.1007/978-981-10-6910-9_6

Kretzschmar, K. and Clevers, H. (2016). Organoids: Modeling development and the stem cell niche in a dish. *Dev Cell 38*, 590-600. doi:10.1016/j.devcel.2016.08.014

LaBarbera, D. V., Reid, B. G. and Yoo, B. H. (2012). The multicellular tumor spheroid model for high-throughput cancer drug discovery. *Expert Opin Drug Discov 7*, 819-830. doi:10.1517/17460441.2012.708334

Lancaster, M. A. and Knoblich, J. A. (2014). Generation of cerebral organoids from human pluripotent stem cells. *Nat Protoc 9*, 2329-2340. doi:10.1038/nprot.2014.158

Lhuissier, E., Bazille, C., Aury-Landas, J. et al. (2017). Identification of an easy to use 3D culture model to investigate invasion and anticancer drug response in chondrosarcomas. *BMC Cancer 17*, 490. doi:10.1186/s12885-017-3478-z

Liu, X., Weaver, E. M. and Hummon, A. B. (2013). Evaluation of therapeutics in three-dimensional cell culture systems by MALDI imaging mass spectrometry. *Anal Chem 85*, 6295-6302. doi:10.1021/ac400519c

Loessner, D., Stok, K. S., Lutolf, M. P. et al. (2010). Bioengineered 3D platform to explore cell-ECM interactions and drug resistance of epithelial ovarian cancer cells. *Biomaterials 31*, 8494-8506. doi:10.1016/j.biomaterials.2010.07.064

Longati, P., Jia, X., Eimer, J. et al. (2013). 3D pancreatic carcinoma spheroids induce a matrix-rich, chemoresistant phenotype offering a better model for drug testing. *BMC Cancer 13*, 95. doi:10.1186/1471-2407-13-95

Lowe, K. A., Chia, V. M., Taylor, A. et al. (2013). An international assessment of ovarian cancer incidence and mortality. *Gynecol Oncol 130*, 107-114. doi:10.1016/j.ygyno.2013.03.026

Markovitz-Bishitz, Y., Tauber, Y., Afrimzon, E. et al. (2010). A polymer microstructure array for the formation, culturing, and high throughput drug screening of breast cancer spheroids. *Biomaterials 31*, 8436-8444. doi:10.1016/j.biomaterials.2010.07.050

Marrella, A., Lagazzo, A., Barberis, F. et al. (2017). Enhanced mechanical performances and bioactivity of cell laden-graphene oxide/alginate hydrogels open new scenario for articular tissue engineering applications. *Carbon N Y 115*, 608-616. doi:10.1016/j.carbon.2017.01.037

Marrella, A., Giannoni, P., Pulsoni, I. et al. (2018). Topographical features of graphene-oxide-functionalized substrates modulate cancer and healthy cell adhesion based on the cell tissue of origin. *ACS Appl Mater Interfaces 10*, 41978-41985. doi:10.1021/acsami.8b15036

Marrella, A., Dondero, A., Aiello, M. et al. (2019). Cell-laden hydrogel as a clinical-relevant 3D model for analyzing neuroblastoma growth, immunophenotype, and susceptibility to therapies. *Front Immunol 10*, 1876. doi:10.3389/fimmu.2019.01876

Marrella, A., Buratti, P., Markus, J. et al. (2020). In vitro demonstration of intestinal absorption mechanisms of different sugars using 3D organotypic tissues in a fluidic device. *ALTEX 37*, 255-264. doi:10.14573/altex.1908311

Modok, S., Scott, R., Alderden, R. A. et al. (2007). Transport kinetics of four- and six-coordinate platinum compounds in the multicell layer tumour model. *Br J Cancer 97*, 194-200. doi:10.1038/sj.bjc.6603854

Nicodemus, G. D. and Bryant, S. J. (2008). Cell encapsulation in biodegradable hydrogels for tissue engineering applications. *Tissue Eng Part B Rev 14*, 149-165. doi:10.1089/ten.teb.2007.0332

Nyga, A., Cheema, U. and Loizidou, M. (2011). 3D tumour models: Novel in vitro approaches to cancer studies. *J Cell Commun Signal 5*, 239-248. doi:10.1007/s12079-011-0132-4

Panczyk, T., Jagusiak, A., Pastorin, G. et al. (2013). Molecular dynamics study of cisplatin release from carbon nanotubes capped by magnetic nanoparticles. *J Phys Chem C 117*, 17327-17336. doi:10.1021/jp405593u

Raghavan, S., Ward, M. R., Rowley, K. R. et al. (2015). Formation of stable small cell number three-dimensional ovarian cancer spheroids using hanging drop arrays for preclinical drug sensitivity assays. *Gynecol Oncol 138*, 181-189. doi:10.1016/j.ygyno.2015.04.014

Sankaranarayanan, R. and Ferlay, J. (2006). Worldwide burden of gynaecological cancer: The size of the problem. *Best Pract Res Clin Obstet Gynaecol 20*, 207-225. doi:10.1016/j.bpobgyn.2005.10.007

Shamir, E. R. and Ewald, A. J. (2014). Three-dimensional organotypic culture: Experimental models of mammalian bi-

ology and disease. *Nat Rev Mol Cell Biol 15*, 647-664. doi:10.1038/nrm3873

Shin, Y., Han, S., Jeon, J. S. et al. (2012). Microfluidic assay for simultaneous culture of multiple cell types on surfaces or within hydrogels. *Nat Protoc 7*, 1247-1259. doi:10.1038/nprot.2012.051

Siegel, R., Naishadham, D. and Jemal, A. (2012). Cancer statistics for Hispanics/Latinos, 2012. *CA Cancer J Clin 62*, 283-298. doi:10.3322/caac.21153

Simian, M. and Bissell, M. J. (2017). Organoids: A historical perspective of thinking in three dimensions. *J Cell Biol 216*, 31-40. doi:10.1083/jcb.201610056

Stock, K., Estrada, M. F., Vidic, S. et al. (2016). Capturing tumor complexity in vitro: Comparative analysis of 2D and 3D tumor models for drug discovery. *Sci Rep 6*, 28951. doi:10.1038/srep28951

Suggitt, M. and Bibby, M. C. (2005). 50 Years of preclinical anticancer drug screening: Empirical to target-driven approaches. *Clin Cancer Res 11*, 971-981.

Talukdar, S. and Kundu, S. C. (2012). A non-mulberry silk fibroin protein based 3D in vitro tumor model for evaluation of anticancer drug activity. *Adv Funct Mater 22*, 4778-4788. doi:10.1002/adfm.201200375

Tang, Y. J., Sun, Z. L., Wu, W. G. et al. (2015). Inhibitor of signal transducer and activator of transcription 3 (STAT3) suppresses ovarian cancer growth, migration and invasion and enhances the effect of cisplatin in vitro. *Genet Mol Res 14*, 2450-2460. doi:10.4238/2015.March.30.3

Tezcan, S., Özdemir, F., Turhal, S. et al. (2013). High performance liquid chromatographic determination of free cisplatin in different cancer types. *Der Pharma Chem 5*, 169-174.

Thoma, C. R., Zimmermann, M., Agarkova, I. et al. (2014). 3D cell culture systems modeling tumor growth determinants in cancer target discovery. *Adv Drug Deliv Rev 69-70*, 29-41. doi:10.1016/j.addr.2014.03.001

Tiwari, A., Krishna, N. S., Nanda, K. et al. (2005). Benign prostatic hyperplasia: An insight into current investigational medical therapies. *Expert Opin Investig Drugs 14*, 1359-1372. doi:10.1517/13543784.14.11.1359

Trujillo-de Santiago, G., Flores-Garza, B. G., Tavares-Negrete, J. A. et al. (2019). The tumor-on-chip: Recent advances in the development of microfluidic systems to recapitulate the physiology of solid tumors. *Materials (Basel) 12*, 2945. doi:10.3390/ma12182945

Weaver, V. M. and Roskelley, C. D. (1997). Extracellular matrix: The central regulator of cell and tissue homeostasis. *Trends Cell Biol 7*, 40-42. doi:10.1016/S0962-8924(97)30078-6

Weeber, F., Ooft, S. N., Dijkstra, K. K. et al. (2017). Tumor organoids as a pre-clinical cancer model for drug discovery. *Cell Chem Biol 24*, 1092-1100. doi:10.1016/j.chembiol.2017.06.012

Xu, X., Farach-Carson, M. C. and Jia, X. (2014). Three-dimensional in vitro tumor models for cancer research and drug evaluation. *Biotechnol Adv 32*, 1256-1268. doi:10.1016/j.biotechadv.2014.07.009

Conflict of interest

SS and MA are cofounders and shareholders of React4life S.r.l. CD and MM are cofounders and shareholders of MTTlab S.r.l.

Acknowledgements

The authors want to thank Paolo Buratti for cell culture support and Francesca Cella for microscopy analysis. This project has received funding from the European Union's Horizon 2020 research and innovation programme under grant agreement No 801159.